Cyclic HMM-based Method for Pathological Gait Recognition from Side View Gait Video

Hoang Xuan Hai, Hoang Le Uyen Thuc

Abstract— The analysis of human gait has become a popular and dynamic research on computer vision. An important application of gait analysis is to early detect the gait abnormalities, which may be caused by some diseases. In this paper, we present a video-based method to recognize common pathological gaits of the elderly such as ataxic, hemiplegic, limping, neuropathic, and Parkinson. There are three main processing steps in the system. In the first step, from each frame of the side view gait video sequence, we first separate the walking person from the background using adaptive background Gaussian Mixture Model. In the second step, we convert the extracted object into a seven-dimensional feature vector based on Hu's moments. In the final step, we analyze those extracted features to recognize different abnormal gaits using Cyclic Hidden Markov Model (CHMM). The Cyclic HMMs are trained with different values of parameters in order to achieve the best reliable recognition model for each disease. Experimental results on simulated abnormal gait database indicate the good performance of the proposed method in terms of low complexity and high recognition rate (about 83% for recognition and 93% for detection task).

Index Terms— Gait analysis, Pathological gait recognition, Gaussian Mixture Model (GMM), Hu's moments, Cyclic Hidden Markov Model (CHMM).

I. INTRODUCTION

The development of science and technology results in the persistent increasing of aging populations, emerging a series of healthcare problems such as chronic diseases on arthritis, cardiovascular, or neurodegenerative diseases. A number of researches conclude that the loss of the ability to walk properly can be a result from a significant health problem, due to the fact that pain, injury, paralysis or tissue damage can alter normal gait [1]. In addition, mental problems can also lead to some gait problems such as gait slowing, which might be a predictor of incident dementia [2]. Thus, a dominant goal of gait analysis is to early detect the gait abnormalities, which may be affected by certain diseases, in order to mitigate their severe consequences.

Pathological gait recognition approaches can be categorized into two main techniques, which are

sensor-based and video-based, depending on the way the data is collected. With today's easy installation, operation and maintenance of a video camera system, it results in the widespread proliferation of video-based method, which concerns the automatic and surreptitious interpretation of human gait from image sequences. In contrast, the sensor-based method is performed in expensive laboratory, requiring a high-structured experimental environment accompanied by trained personnel and is intrinsic intrusiveness.

In recent years, there have been a series of research projects all over the world on video-based solutions for pathological gait recognition. For example, the study by Liao et al. [3] analyzes the walking posture from side-view and front-view videos. Four features extracted from the segmented silhouette of walking human are bodyline, neckline, center of gravity (COG) and base width. Tilting angles associated with body and necklines and their periodic variation are adopted to evaluate upper body posture. The COG and gait width features are used to evaluate the posture condition of lower body parts. The system achieves acceptable performance with low cost and high convenience. The paper by Stone and Skubic [4] presents initial results of continuous monitoring the gait of elderly residents in an independent living facility, using the depth camera Microsoft Kinect. Instead of using the Kinect skeletal tracking, they process the raw disparity values from the Kinect depth streams to achieve further distance working range (up to 8 meters) and more accurate gait measurement. Paolo et al. [5] propose a video-based portable tool for clinical gait analysis by processing a video stream by tracking different markers placed in five specified points of the subject's leg. To deal with occlusions, they apply Kalman filter in conjunction with Mahalanobis distance for correcting and interpolating the estimation. Experimental results show that the system is able to reconstruct marker position and leg kinematics even if occlusions occur.

Most of the existing video-based pathological gait detection systems use either multiple cameras (e.g., two cameras) or depth camera or combine camera(s) and markers. In this paper, we propose a simpler video-based system for recognition of popular diseases which result in gait abnormality in elderly. The proposed system uses only one conventional camera to record the movements of the subject in side view. Unlike the other method [3, 5], in our system, the gait disorders can be detected without tracking or recognizing limbs or body parts. In addition, the

quasi-periodicity property of human walking increases the difficulty level of the recognition task, due to the fact that the motion from one cycle to the next is not perfectly repeated. By using the variation of Hidden Markov Model (HMM), which is Cyclic HMM, the characteristics of quasi-periodic human motions can be effectively captured. Finally, researches on this branch have almost focused their attention on the problems such as detecting unusual gait [6] or estimating the gait parameters [3, 4]. In this study, the gait analysis is considered from a different aspect. It can be used as a means to deduce certain disease related to gait disorder of people.

The rest of the paper is organized as follow: in Section II, we generally describe the overview of the proposed methodology. The processing steps in the system are then presented in Section III with more details. Experimental results are shown in Section IV, followed by conclusion in Section V.

II. OVERVIEW OF THE PATHOLOGICAL GAIT

Human gait analysis can be simply described as the study of human locomotion by measuring body movements, body mechanics, and the activities of muscles. Actually people can move in many ways such as running, hopping, skipping, or even crawling; however, like most gait analysis researches, in this study, we only attend to walking gait. Section II begins by presenting the specific parameters associated with normal gait, so we can understand the abnormality. After that, the diseases that are considered in our work are carefully described.

A. Gait parameters

Basically, there are three main gait parameters:

1) *Step length* is the distance from the heel of one foot to the next heel of the opposite foot, as in Fig. 1. Normally, step length tends to decrease with age, pain and disease. A healthy person has the same step lengths for both legs, resulting in the smooth rhythm of walking [7]. The step length is closely related to the *gait cycle,* which is the total length of two continuous steps. There are two major phases in a gait cycle, i.e., *stance phase* and *swing phase*. Stance phase is when the foot is on the ground and swing phase is when the foot is on the air swinging to forward. Most problems related to lower limbs could be observed clearly in the stance phase.

2) *Base* (or step width) is the distance between two feet during walking [7] as in Fig. 1. Base should be shoulder length or a little less and should remain relatively stable from step to step. Normally, the wider base width is due to some pathology, which decrease the ataxic balance. The smaller or the crossover base width in some cases could be a warning sign of an imminent fall or a symptom of gait disorders.
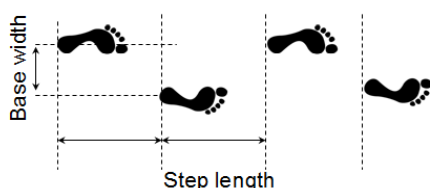

Figure 1.   Illustration of step length and base width.

3) *Gait speed* is the distance a person can travel in a certain amount of time. There are some factors, which affect gait speed, such as age, sex, step length, and health status, etc. In addition, gait speed is significantly influenced by health condition.

B. Common pathological gait disorders in the elderly

Normally, walking gait declines with non-pathological aging, involving stooped posture, reduced arm swing, reduced step length, reduced gait speed and a tendency towards a flat foot strike. However, musculoskeletal and neurological diseases can attribute to this normal decline, causing the reduced quality of life and the increased risk of fall [1].

In this paper, we focus on recognizing common gait disorders in the elderly. They are ataxic, hemiplegic, limping, neuropathic, and Parkinson. The description of such gaits is in the following,

1) *Ataxic gait* is most commonly seen in cerebellar disease. The gait of an intoxicated person also resembles ataxic gait. This gait can be either observed in severe reduction proprioception. The patient's gait is usually wide or variable base, reduced or variable step length, loosed balance, irregular lurching steps, and abducted arms [1].

2) *Hemiplegic gait* is the typical gait of patients with upper motor neuron lesion. This gait is most commonly seen in stroke. The patient has unilateral weakness with the upper extremity in flexion and lower extremity in extension. When walking, the patient holds his arm to one side and drags his affected leg in a semicircle, due to the weakness of distal muscles and extensor hypertonia in lower limb [1].

3) *Limping gait* has many causes. These include injuries such as muscle strains, injured ligaments, etc., infections such as septic arthritis, osteomyelitis, or developmental problems such as muscular dystrophy, different leg lengths, etc. The patient is walking irregularly with hobbling, pain or discomfort. They usually put uneven pressure on two foot.

4) *Neuropathic gait* is most often seen in peripheral nerve disease. The cause of this gait is the weakness of foot dorsiflexion. The patient has to walk with the high lifted leg so that the toes do not drag on the floor [1].

5) *Parkinson gait* is the most common abnormal gait in the elderly. This gait is seen in Parkinson patient or any other condition causing Parkinsonism, such as side effect from drugs. This gait is characterized by a small step length, stooped posture, slow gait speed, reduced arm swing, lack of pivot during turning and poor balance [1].

III. PROPOSED SYSTEM

Our designed system aims to observe the elderly walking in the indoor environment with almost static background and/or corridor with acceptable lighting condition for gait abnormality recognition. In order to provide video stream for the entire system, we install a single cheap conventional camera in the suitable place so that we can capture the video of one person walking in side view and then transmit to the computer for gait analysis.

The basic architecture of our system is shown in Fig. 2.

The system follows three stages of operations: object segmentation, feature extraction and pathological gait recognition. First, the human object is segmented frame-by-frame from the background of image by using the adaptive GMM; second, segmented object is converted into seven-dimensional feature vector based on Hu's seven moments; and finally, specified pathological gait is identified among other defined pathological gaits by Cyclic HMM.
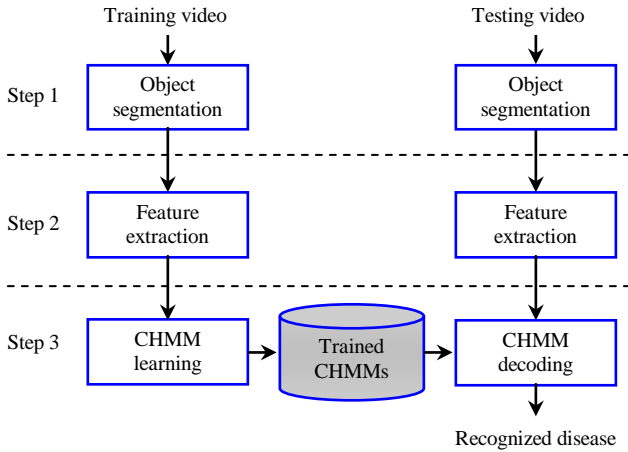

Figure 2.   Three basic processing steps of the proposed pathological gait recognition system.

The details of three processing steps will be presented in the following,

A. Human object segmentation

Adaptive background GMM approach [8] is very common to distinguish walking human from the background.

At time *t*, the value of pixel at (x_0, y_0) in frame is X_t. The sequence of each pixel, $\{X_1, ..., X_t\}$, is constructed by a Gaussian Mixture Model with K components. The probability of observing the current pixel value is calculated by,

$$p(X_t) = \sum_{i=1}^{K} w_{i,t}\, \eta(X_t, m_{i,t}, \Sigma_{i,t})$$
(1)

where $\omega_{i,t}$ is an estimated weight of the ith Gaussian distribution at time t, η is the pdf of ith Gaussian distribution, $\mu_{i,t}$ is the mean value of the ith Gaussian at time *t*, and $\Sigma_{i,t}$ is the covariance matrix of the ith Gaussian at time *t*.

Every new pixel value is checked against K existing Gaussian distributions, until a match (pixel value within 2.5 standard deviations of a distribution) is found [8].

When none Gaussian is matched, X_t is marked as a foreground pixel and the least probable component is replaced by a distribution with the current value as its mean, an initial high variance, and a low weight parameter.

As the parameters of the mixture model of each pixel change, the Gaussians are reordered by the value of ω/σ then the first BG distributions are chosen as the background model, where

$$BG = \arg\min_b \left(\sum_{k=1}^{b} w_k > T \right)$$
(2)

where T is the minimum fraction of the background model.

In this study, we use improved GMM for object segmentation [9]. This algorithm uses recursive equations to constantly update the parameters and to simultaneously select the appropriate number of Gaussian components for each pixel.

After extracting the human object, some morphological operations such as closing and opening are implemented to smooth the boundary and fill the small holes to create proper silhouette images.

Finally, in order to avoid the large size of image, we use detector window where its center is the centroid of the object blob to create a Region Of Interest (ROI) around the object and remove the pixels outside it.

The results of human object segmentation process are shown in Fig. 3. Here, a big hole in lower leg in silhouette (Fig. 3a) is filled after morphology process (Fig. 3c).
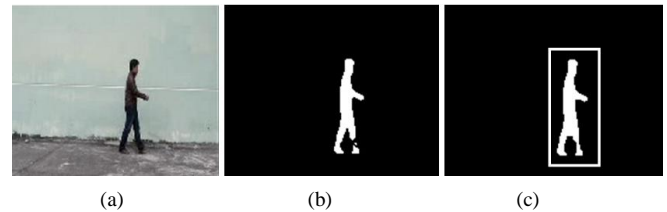

(a)   (b)   (c)

Figure 3.   (a) Original image, (b) Segmented silhouette by improved GMM, (c) Segmented silhouette after morpological operations with ROI.

B. Feature extraction

The silhouette image in each frame will be transformed into a reduced representation set of features. The chosen feature descriptor in this study is based on Hu's seven moments, due to their advantageous characteristics in statistical describing geometric figures [10]. Specially, Hu's moments can effectively describe the binary silhouettes, regardless of their size, location, and orientation in image frames.

These moments are calculated based on two-dimensional moments:

$$m_{pq} = \int \int x^p y^q \, \rho(x,y)\,dxdy$$
(3)

where $\rho(x,y)$ is the binary image:

$$\rho(x,y) = \begin{cases} 1 & \text{if } (x,y) \notin \text{silhouette} \\ 0 & \text{if } (x,y) \notin \text{background} \end{cases}$$
(4)

The above 2D moments can be made to be invariant to translation by central moments, which are defined as follows:

$$\mu_{pq} = \int \int (x - \bar{x})^p (y - \bar{y})^q \, \rho(x,y)\,dxdy$$
(5)

where pixel point $(\bar{x}, \bar{y})$ is the centroid of the binary image:

$$\bar{x} = \frac{m_{10}}{m_{00}} \text{ and } \bar{y} = \frac{m_{01}}{m_{00}}$$
(6)

Next, we can make central moments to be scale invariance by normalization and get the normalized central moments as in the following:

$$\eta_{pq} = \frac{\mu_{pq}}{\mu_{00}^{\frac{p+q}{2}+1}}$$
(7)

Finally, in order to obtain the features invariant to the rotation of image, based on normalized central moments, we calculate following seven Hu's moments as in [10]:

$$S_1 = \eta_{20} + \eta_{02}$$
$$S_2 = (\eta_{20} - \eta_{02})(\eta_{20} - \eta_{02}) + 4\eta_{11}\eta_{11}$$
$$S_3 = (\eta_{30} - 3\eta_{12})(\eta_{30} - 3\eta_{12}) + (\eta_{03} - 3\eta_{21})(\eta_{03} - 3\eta_{21})$$
$$S_4 = (\eta_{30} + \eta_{12})(\eta_{30} + \eta_{12}) + (\eta_{03} + \eta_{21})(\eta_{03} + \eta_{21})$$
$$S_5 = (\eta_{30} - 3\eta_{12})(\eta_{30} + \eta_{12})[(\eta_{30} + \eta_{12})(\eta_{30} + \eta_{12}) - 3(\eta_{03} + \eta_{21})(\eta_{03} + \eta_{21})]$$
$$+ (3\eta_{21} - \eta_{03})(\eta_{03} + \eta_{21})[3(\eta_{30} + \eta_{12})(\eta_{30} + \eta_{12}) - (\eta_{03} + \eta_{21})(\eta_{03} + \eta_{21})]$$
$$S_6 = (\eta_{20} - \eta_{02})[(\eta_{30} + \eta_{12})(\eta_{30} + \eta_{12}) - (\eta_{03} + \eta_{21})(\eta_{03} + \eta_{21})]$$
$$+ 4\eta_{11}(\eta_{30} + \eta_{12})(\eta_{03} + \eta_{21})]$$
$$S_7 = (3\eta_{21} - \eta_{03})(\eta_{30} + \eta_{12})[(\eta_{30} + \eta_{12})(\eta_{30} + \eta_{12}) - 3(\eta_{21} + \eta_{03})(\eta_{21} + \eta_{03})]$$
$$- (\eta_{30} - 3\eta_{12})(\eta_{21} + \eta_{02})[3(\eta_{30} + \eta_{12})(\eta_{30} + \eta_{12}) - (\eta_{21} + \eta_{03})(\eta_{21} + \eta_{03})]$$

(8)

Since the values of Hu's moments, especially from S_2, are extremely small, we propose to take the logarithm of moments so that their values are larger to avoid possible unexpected errors when computing the so-closely small numbers. This was proven through experiments either: original Hu's moments give the poor recognition rate. In our study, Hu's moments can be negative somehow; hence, we have to calculate the logarithm of absolute of seven moments. Thus, the above proposed transform has mapped the so-closed Hu's moments into the new space, where the different feature vector points keep apart large enough to be reliably processed. Fig. 4 is the binary image and its corresponding original and transformed Hu's moments.

	Original moments	Transformed moments
S_1	0.34612098	-1.060966902
S_2	0.07375973	-2.606942324
S_3	0.00930633	-4.677060365
S_4	0.00423419	-5.464563289
S_5	2.61E-05	-10.55229091
S_6	0.00106340	-6.846275116
S_7	4.85E-06	-12.23698935

Figure 4.   Original binary image and its seven corresponding orignal and transformed moments.

C. Pathological gait recognition

After being transferred to sequence of feature vectors from previous stages, video data need to be analyzed for pathological gait recognition. In our system, we employ HMM to achieve this goal. Intuitively, walking action exhibit quasi-periodicity, where the motion from one cycle to the next is not perfectly repeated and the number of cycles is not a predefined value. This motivates our use of Cyclic HMM (CHMM) [11] – a variation of left-to-right structure with a return transition from the ending state to the beginning state, so as to be able to model the walking actions with quasi-periodicity characteristics.

There are two main types of HMM which are discrete HMM and continuous HMM. Four our implementation, we do not use discrete version to avoid the quantization distortion created by the vector quantization process when we build the codebook containing the observed symbols of the model.

One limitation of HMMs is that the feature vector sequence (i.e., the sequence of observed symbols) is only well modeled if the parameters of HMMs are appropriate chosen. Unfortunately, to our best knowledge, there is still no systematic method to optimally choose the HMM parameters.

Therefore, we have to conduct a number of experiments to achieve the best reliable models for our application.

Fig. 5 is an example of continuous CHMM used in our system.

The use of CHMM covers two phases, which are training and testing. The data used to feed CHMM is from self-built stimulated pathological gait videos. The whole database is divided into two sets for training and testing.

1)   The *training process* is carried out by building six CHMMs (each model is to model one type of gait abnormality in the database) to optimize the corresponding state transition matrices *A*s and observation probability distributions *B*s. In the continuous case, *B* is given by the parameters of the *probability density function* (pdf) of the observation vector at time *t* given the state of the model. The Gaussian distribution is selected to represent these pdfs. The training process is performed by the Baum-Welch algorithm [12] to derive the *maximum likelihood* (ML) estimation of the model parameters $\lambda = \{A, B, \pi\}$. The training algorithm is run until convergence condition is satisfied. If it runs over *10.000* times without convergence, it will be forced to stop.
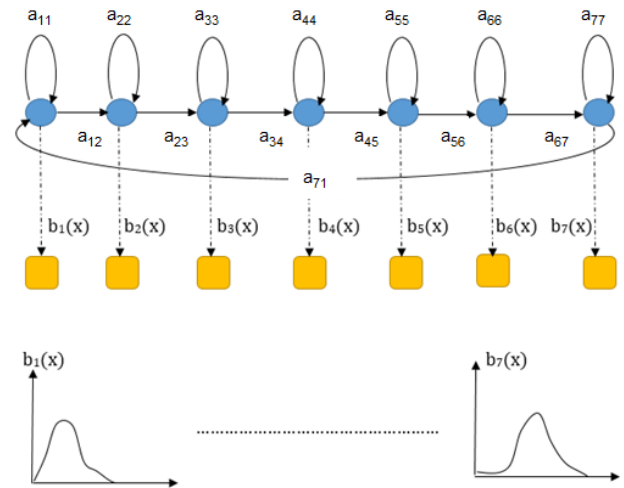
Figure 5.   Seven-state continuous CHMM.

2) The *testing process* is the construction of a ML classifier as depicted in Fig. 6. Given a sequence of feature vectors from testing video data, we compute the likelihoods that the trained CHMMs generating this testing sequence. Finally, in the decision step, we select the CHMM that has the ML to be the corresponding class of testing gait.
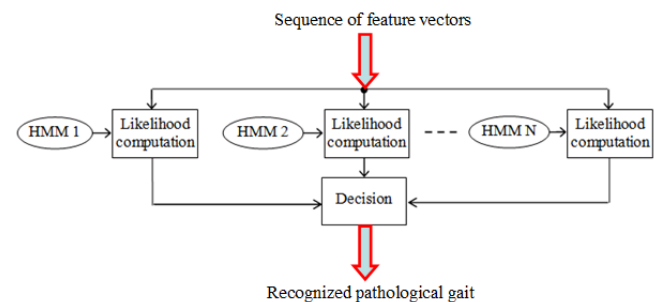
Figure 6.   ML classifier.

IV. SYSTEM EVALUATION

The evaluation of the video analysis algorithm used in this system is performed through a self-built simulated normal/abnormal gait database. Two main experiments are done: in the first experiment, we do compare the discrete and continuous CHMM in recognizing the abnormal gaits. In the second experiment, we try to choose the appropriate CHMM parameters through several sub-experiments. Both experiments use the completely different training and testing data captured from different people. The performance of the system is measured by the recognition rate, using ten-fold cross validation rule.

A. Self-built database

Each of the ten volunteers is instructed to perform a set of predefined walking actions including normal walk, ataxic, hemiplegic, limping, neuropathic, and Parkinson as described in [1]. The volunteers have various genders, ages, weights, and heights. Each type of gait is performed multiple times by multiple people in various speeds. Volunteers' clothes and hairstyle are at their convenience. These help the database to be diverse and challenging.

In total, we collect 56 ataxic, 85 hemiplegic, 93 limping, 97 neuropathic, 97 Parkinson, and 101 normal walk videos. All videos are compressed in .avi format with the size of 180x144, and recorded by a cheap conventional camera in a corridor under relatively good lighting conditions.

Fig. 7 shows some images of pathological gaits in the database.

Figure 7. Image frames of gaits in the database (from the top row the the bottom: ataxic, hemiplegic, limping, neuropathic, Parkinson, and walk).

B. Experiment 1

In this experiment, we try to validate what was analyzed in Section III_C about quantization distortion discrete HMM by performing several experiments on both discrete and continuous HMM. All CHMMs used have the same number of hidden states. For discrete CHMM, the size of the codebook is *32*, *64*, and *128* in sequence. Table I is the total recognition result of this experiment with the codebook size of *128*, showing that the continuous CHMM is always dominant.

TABLE I.   RECOGNITION RATE OF DISCRETE VS. CONTINUOUS HMM

	N = 7	**N = 9**
Discrete HMM	74.23%	74.83%
Continuous HMM	76.76%	79.33%

C. Experiment 2

In this experiment, in order to choose the proper CHMM parameters, we perform 9 sub-experiments with the number of hidden states within the range [3-11]. Table II presents the recognition rate measured in % through these *9* experiments.

TABLE II.   RECOGNITION RATE (%) OF SYSTEM THROUGH 9 EXPERIMENTS

N	Atax	Hemi	Limp	Neur	Park	Walk	Total
3	65.5	49.3	87	52.1	99	78	71.82
4	67.3	52.1	80.4	58.3	97.9	77	72.16
5	65.5	55.1	82.6	56.2	97.9	81	73.05
6	67.3	56.6	92.4	56.2	97.9	77	74.57
7	67.3	52.1	95.7	62.5	99	84	76.77
8	72.7	54.9	73.9	70.8	96.9	83	75.37
9	74.5	62.9	83.7	69.8	99	85	79.15
10	70.9	70.5	89.1	76	99	80	80.92
11	76.4	73.1	87	72.9	99	72	80.07

Based on the results of previous experiments, the numbers of states of six models are chosen differently so as to achieve the most reliable model for each gait. Specifically, they are *7* for limping, neuropathic, Parkinson, walking, *9* for ataxic, and *10* for hemiplegic.

The recognition rate of the experiment through CHMMs with different number of states is shown in Table III. The overall recognition rate is nearly *83%*, providing the reasonably good performance.

TABLE III.   RECOGNITION RATE (%) OF SYSTEM THROUGH CHMMS WITH DIFFERENT NUMBER OF STATES

	Atax	**Hemi**	**Limp**	**Neur**	**Park**	**Walk**
Atax	**74.5**	12.7	1.8	7.3	0	3.6
Hemi	7.6	**68.4**	11.4	0	0	12.7
Limp	0	5.4	**92.4**	0	0	2.2
Neur	0	6.2	9.4	**76**	0	8.3
Park	1	0	0	0	**99**	0
Walk	7	4	2	2	0	**85**
Total	82.55					

By using the deployed pathological gait recognition algorithm, we can apply it for abnormal gait detection, which is a special case of abnormal gait recognition. From Table III, we get the remarkable statistical results [13] of abnormal gait detection task as in the following,

$$\mathrm{Re}\,call = \frac{TP}{TP+FN} = 94.64\%$$

$$\mathrm{Pr}\,ecision = \frac{TP}{TP+FP} = 91.88\% \qquad (9)$$

$$Accuracy = \frac{TP+TN}{TP+TN+FP+FN} = 93.03\%$$

where True Positive (TP) is the number of abnormal gaits which are correctly detected, False Positive (FP) is the number of normal gaits which are incorrectly recognized to be abnormal, True Negative (TN) is the number of normal gaits which are correctly recognized, and False Negative (FN) is the number of abnormal gait which are not detected.

Besides the good performance, it is possible to mention another advantage of our system; that is, the system only requires using very short videos to perform the recognition/detection task. In our experiments, 42 seconds and 10 seconds are the maximum and minimum video lengths, respectively.

V. CONCLUSION

In this paper, we have proposed a system for recognition of common pathological gaits of the elderly from side view gait video. Segmentation of human object by adaptive background GMM followed by suitable morphological operations helps to provide well-defined silhouettes. With the use of features based on Hu's seven moments, the shape of abnormal gaits can be interpreted without tracking limbs or body parts. By exploiting the continuous Cyclic HMMs, the system has the capability to classify pathological gaits, regardless of the quasi-periodic nature of walking action, which results in the high difficulty of recognition task. Initial results in experiments on simulated abnormal gait database show that the capability of the designed system is promising in recognizing as well as detecting several pathological gaits. In our future researches, we are going to apply three-dimensional and temporal features to make the system view-invariant and more accurate.

REFERENCES

[1] Joseph H. Friedman, "Gait Disorders in the Elderly," *Medicine & Health*, vol. 95[3], pp. 84-85, 2012.
[2] L. M. Waite, D. A. Grayson, O. Piguet, H. Creasey, H. P. Bennett, G. A. Broe, "Gait Slowing as a Predictor of Incident Dementia: 6-year longitudinal data from the Sydney Older Persons Study," *Journal of the Neurological Sciences*, pp. 89-93, 2005.
[3] Tsung-Yen Liao, Shaou-Gang Miaou, and Yu-Ren Li, "A Vision-based Walking Posture Analysis System without Markers," *2nd Int. Conf. on Signal Processing Systems*, pp. 254-258, 2010.
[4] Erik E. Stone and Marjorie Skubic, "Passive, In-home Gait Measurement Using an Inexpensive Depth Camera: Initial Results," *6th Int. Conf. on Pervasive Computing Technologies for Healthcare and Workshops*, pp. 183-186, 2012.
[5] Paolo Soda, Alfonso Carta, Domenico Formica, and Eugenio Guglielmelli, "A low-cost video-based tool for clinical gait analysis," *31st Annual Int. Conf. of the IEEE EMBS*, pp. 3979-3982, 2009 .
[6] Christian Bauckhage, John K. Tsotsos, and Frank E. Bunn, "Detecting abnormal gait," *2nd Canadian Conf. on Computer and Robot Vision*, pp. 282-288, 2005.
[7] http://thephysiotherapy.com/normal-parameters-of-gait/
[8] C. Stauffer and W.E.L. Grimson, "Adaptive background mixture models for real-time tracking," *IEEE Conf. of Computer Vision and Pattern Recognition*, vol. 2, pp. 246-252, 1999.
[9] Z. Zivkovic, "Improved adaptive Gaussian mixture model for background subtraction," *17th Int. Conf. on Pattern Recognition (ICPR)*, pp. 28-31, 2004.
[10] Zhihu Huang and Jinsong Leng, "Analysis of Hu's Moment Invariants on Image Scaling and Rotation," *2nd Int. Conf. on Computer Engineering and Technology (ICCET)*, pp. 476-480, 2010.
[11] Hoang Le Uyen Thuc, Shian-Ru Ke, Jenq-Neng Hwang, Pham Van Tuan, and Truong Ngoc Chau, "Quasi-periodic Action Recognition from Monocular Videos via 3D Human Models and Cyclic HMMs," *Int. Conf. on ATC*, pp. 110-113, 2012.
[12] Lawrence R. Rabiner, "A tutorial on hidden Markov models and selected applications in speech recognition," *Proc. IEEE*, vol. 77(2), pp. 257-286, 1989.
[13] T. Fawcett, "ROC Graphs: Notes and Practical Considerations for Researchers," 2004.